Expression of Insulin System in the Olfactory Epithelium: First Approaches to its Role and Regulation

Article *in* Journal of Neuroendocrinology · September 2008

DOI: 10.1111/j.1365-2826.2008.01777.x · Source: PubMed

11 authors, including:

Marie-Christine Lacroix
French National Institute for Agricultural R…
32 PUBLICATIONS **752** CITATIONS
SEE PROFILE

Nicolas Meunier
French National Institute for Agricultural R…
27 PUBLICATIONS **492** CITATIONS
SEE PROFILE

Christine Baly
French National Institute for Agricultural R…
37 PUBLICATIONS **874** CITATIONS
SEE PROFILE

Patrice Congar
French National Institute for Agricultural R…
35 PUBLICATIONS **1,255** CITATIONS
SEE PROFILE

Journal of Neuroendocrinology
From Molecular to Translational Neurobiology

Journal of Neuroendocrinology **20**, 1176–1190

ORIGINAL ARTICLE

Expression of Insulin System in the Olfactory Epithelium: First Approaches to its Role and Regulation

M.-C. Lacroix,*†‡ K. Badonnel,*†‡ N. Meunier,*†‡§ F. Tan,¶ C. Schlegel-Le Poupon,† D. Durieux,*†‡ R. Monnerie,*†‡ C. Baly,*†‡ P. Congar,*†‡ R. Salesse*†‡ and M. Caillol*†‡

**INRA, UMR 1197 Neurobiologie de l'Olfaction et de la Prise Alimentaire, Recepteurs et Communication Chimique, Jouy en Josas, France.*

†INRA, UMR 1197 Neurobiologie de l'Olfaction et de la Prise Alimentaire, Biochimie de l'Olfaction et de la Gustation, Jouy en Josas, France.

‡Université Paris-Sud, UMR1197, Orsay, France.

§Université de Versailles Saint Quentin en Yvelines, Versailles, France.

¶INSERM U564, Equipe AVENIR, Cytokines: Structure and Signalisation Tumorale, Angers, France.

Journal of Neuroendocrinology

Food odours are major determinants for food choice; their detection is influenced by nutritional status. Among different metabolic signals, insulin plays a major role in food intake regulation. The aim of the present study was to investigate a potential role of insulin in the olfactory mucosa (OM), using *ex vivo* tissues and *in vitro* primary cultures. We first established the expression of insulin receptor (IR) in rat olfactory mucosa. Transcripts of IR-A and IR-B isoforms, as well as IRS-1 and IRS-2, were detected in OM extracts. Using immunocytochemistry, IR protein was located in olfactory receptor neurones, sustentacular and basal cells and in endothelium of the lamina propria vessels. Moreover, the insulin binding capacity of OM was quite high compared to that of olfactory bulb or liver. Besides the main pancreatic insulin source, we demonstrated insulin synthesis at a low level in the OM. Interestingly 48 h of fasting, leading to a decreased plasmatic insulin, increased the number of IR in the OM. Local insulin concentration was also enhanced. These data suggest a control of OM insulin system by nutritional status. Finally, an application of insulin on OM, aiming to mimic postprandial insulin increase, reversibly decreased the amplitude of electro-olfactogramme responses to odorants by approximately 30%. These data provide the first evidence that insulin modulates the most peripheral step of odour detection at the olfactory mucosa level.

Key words: rat olfactory mucosa, insulin-receptor, insulin, electro-olfactogramme.

doi: 10.1111/j.1365-2826.2008.01777.x

Correspondence to:
Marie-Christine Lacroix, INRA, UMR 1197 Neurobiologie de l'Olfaction et de la Prise Alimentaire, Recepteurs et Communication Chimique, F-78350 Jouy en Josas, France (e-mail: marie-christine.lacroix@jouy.inra.fr).

Animals are known to regulate their body weight through a complex homeostatic mechanism. The control of food intake plays a crucial role in these regulations and is mainly ensured by the hypothalamus. To achieve this control, the hypothalamus receives inputs from circulating factors, and from external signals transmitted by sensory organs, such as food availability and quality (1). Insulin is one of the most important metabolic signals between the endocrine system and the brain. Previous studies in the baboon reported that the intracerebroventricular administration of insulin decreased food intake, whereas, in mice, the selective deletion of insulin receptors (IR) in neurones resulted in hyperphagia leading to obesity (2). IR are widely distributed throughout the central nervous system, with a high level of expression being observed in the cortex, hippocampus, hypothalamus and olfactory bulbs (3). IR expression in the olfactory bulb suggests that insulin may in part regulate food intake by modulating the olfactory message. Indeed, food odours are among the major determinants for food choice and intake. Conversely, the nutritional status of individuals influences odour detection. In primates and humans, fasting results in an increased perception of some food-related odours (4), whereas satiety regarding one type of food is correlated with a reduction in olfactory detection specific to this food (5). Odours signals are processed through multiple steps starting in the olfactory mucosa (OM) and then reaching the olfactory bulb, before being integrated in different areas of the central nervous system. To date, the neural bases for these olfactory performance modulations by the nutritional status have been only identified in the olfactory bulb, at the level of mitral cells (6), the projections of which constitute the principal

output of the olfactory bulb. Among the nutritional signals, insulin has been shown to act at the level of olfactory bulb. The response of mitral cells to odours is mostly increased after a subcutaneous insulin injection (7), and more recent studies have established that insulin modulates the electrical activity of olfactory bulb neurones through phosphorylation of the voltage-gated ion channel Kv1.3 (8). However, the olfactory bulb only comprises the second level of odour detection. Data obtained in our laboratory suggest that metabolic status could also control the first level of odour detection. Leptin, orexins and their receptors are expressed in the OM (9, 10). Interestingly, fasting causes a significant enhanced transcription of both leptin and its receptors (10). Moreover, fasting also modulates the expression of a subset of transcripts in the OM, some of which, such as the odorant-binding protein 1F, are involved in odour detection (11). In view of these data, we decided to investigate the presence and localisation of insulin receptor in the OM, its role and possible regulation.

The OM consists of a pseudostratified neuroepithelium (olfactory epithelium, OE) that lies on a lamina propria (Fig. 1). The OE is composed of olfactory receptor neurones (ORNs) interspersed with non-neuronal sustentacular cells (SUS). Olfactory receptors are expressed on cilia of the dendritic knobs of ORNs. Throughout life, ORNs and SUS are renewed through the proliferation of horizontal (HBC) and globose basal cells (GBC), located at the base of the OE (12). The lamina propria is composed of Bowman's glands, blood vessels, fibroblasts and ORNs axons wrapped in ensheathing cells. First, we checked the expression of the insulin receptor in the different OM cell types, the occurrence of its two variant types (IR-A and IR-B) (13), its level of expression, localisation and insulin binding capacity. We also examined a possible local insulin production by the OM. Finally, we checked whether the modification of the nutritional status influenced insulin system expression in the OM, and whether insulin application on this tissue was able to modulate the responses of ORNs to odorants.

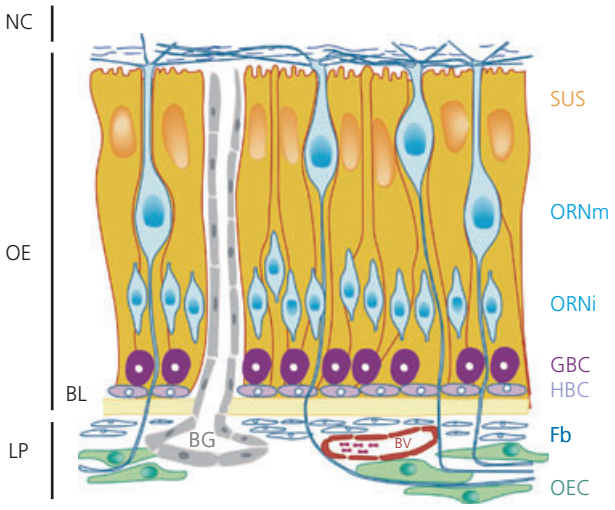

Fig. 1. Schematic representation of the olfactory mucosa (OM). OM lines the dorsal aspect of the nasal cavity (NC). OM consists of a pseudostratified epithelium (OE) and a lamina propria (LP), separated by a basal lamina (BL). The upper compartment of the OE, toward the NC, is composed of sustentacular cells (SUS) and mature olfactory receptor neurones (ORNm). The medium part consists of immature ORN (ORNi) and the basal part of globose cells, horizontal basal cells (GBC and HBC, respectively) and SUS end feet. Lamina propria is composed of olfactory ensheathing cells (OEC), fibroblasts (Fb), Bowman's gland (BG) and blood vessels (BV).

Materials and methods

Reagents

Antibodies directed against the following antigens were used: human CK14 (mouse monoclonal, clone LL002; Biogenex, San Ramon, CA, USA), CK18 (mouse monoclonal, clone RGE 53; Servibio, Meudon, France), β-tubulin isotype III (mouse monoclonal, clone SDL.3D10; Sigma Aldrich, Saint-Quentin Fallavier, France), bovine/porcine insulin (rabbit polyclonal antibody, Immunostar; Euromedex, Mundolsheim, France), human insulin-receptor β [IRβ immunocytochemistry: rabbit polyclonal antibody ab10991 (Abcam, Cambridge, UK) or rabbit polyclonal antibody sc-711 (Santa-Cruz, Tebu, Le Perray-en-Yvelines, France); western: rabbit polyclonal antibody sc-711], insulin receptor substrate-1 and -2 (IRS-1, IRS-2; rabbit polyclonal antibodies; Santa-Cruz), human Pdx1 (rabbit polyclonal antibody kindly supplied by Dr R. Scharfmann, INSERM, Paris, France) (14) and globose basal cells (GBC2 antibody) kindly supplied by Dr J. E. Schwob (Tufts University School of Medicine, Boston, MA, USA) (15). Labelling were visualised using fluorescent secondary antibodies obtained from Molecular Probes (Alexa 488-conjugated goat anti-mouse, Alexa 488-conjugated goat anti-rabbit, Alexa 555-conjugated donkey anti-mouse, Alexa 555-conjugated donkey anti-rabbit; Invitrogen, Cergy Pontoise, France) or an avidin-biotin-peroxidase kit (ABC Elite, Vectastain, Abcys, Paris, France). Control sera were obtained from Jackson ImmunoResearch Laboratories (West Grove, PA, USA) and mouse IgG1 and IgG2b controls came from Immunotech (Marseille, France). Modified Eagle's Joklic medium, collagen type IV, L-ascorbic acid 2-phosphate and bovine insulin were obtained from Sigma Aldrich and RDB from Euromedex. Dulbecco's modified Eagle's medium/Ham F-12 (F12/DMEM) low glucose (1.4 g/l) and newborn calf serum (NCS) came from Eurobio (Courtaboeuf, France). Dispase II (2.4 U/ml) was obtained from Roche Diagnostics (Meylan, France). Recombinant Human Epidermal Growth Factor (EGF), GlutaMAX, penicillin/streptomycin and Trizol Reagent were obtained from Invitrogen. The rat insulin radioimmunoassay (RIA) kit came from Linco Research Millipore (Saint-Quentin en Yvelines, France).

Experimental animals

All animal experiments were conducted in accordance with the European Communities Council Directive of 24 November 1986 (86/609/EEC). Every effort was made to minimise the number and suffering of rats. Experiments were carried out on young (1–3 weeks) or adult (2–3 months) male Wistar rats born in our laboratory. They were kept under controlled conditions of light (12 : 12 h light/dark cycle, lights on 08.00 h) and temperature (22 °C) with free access to pellet food (M25; Dietex, Saint-Gratien, France) and tap water. To determine the effect of fasting, control rats were fed between 17.00 h and 08.00 h. For starved rats, food but not water was withheld for 48 h. For all experiments rats were killed at the beginning of the light phase (08.00–11.00 h) by decapitation, which was properly conducted by skilled staff using well-maintained equipment, ensuring rapid death. The OM and control tissues (olfactory bulb, pancreas, liver and kidneys), were rapidly collected and either frozen in liquid nitrogen for RNA and protein extraction or incubated in Dispase solution for the culture of OE cells. For fasting experiments, blood was collected and plasma was stored for later analysis of insulin levels.

Primary culture of olfactory epithelium

Adult rats were deeply anaesthetised with sodium pentobarbital (CEAV, Libourne, France; 100 mg/kg) and killed by decapitation. To prevent contamination by the respiratory epithelium, we only collected nasal septum epithelium. The OE was cultivated as previously described with few modifications (16). Briefly, after 45 min of incubation in 2.4 U/ml Dispase II solution at 37 °C, the olfactory epithelium was carefully separated from the lamina propria. Epithelial fragments were then gently triturated to separate the cells mechanically. Cell suspensions from different animals were pooled in a 15-ml conical tube and F12/DMEM was added. The cell suspension was centrifuged and the pellet re-suspended in a culture medium composed of F12/DMEM containing NCS (10%), GlutaMAX (2 mM), penicillin (10 U/ml), streptomycin (10 μg/ml) and L-ascorbic acid 2-phosphate (200 μM). Medium supplementation with insulin, as described in Feron *et al.* (16), was omitted. Each rat epithelium yielded approximately 1.5 million cells. Cells were plated in four-well NUNC culture plates on 15-mm sterile glass coverslips coated with collagen IV (5 $\mu g/cm^2$) and placed at 37 °C in a humidified atmosphere of 5% CO_2 in air. The equivalent of one rat epithelium was equally distributed in a four-well culture plate. The culture medium was changed every 48 h. EGF (25 ng/ml) was added to the culture medium only from the fourth day of culture, to promote the development of non-neuronal cells. Cultures were stopped after 2 or 10 days of culture, and the cells were either fixed for 20 min at room temperature in paraformaldehyde L-lysine metaperiodate (PLP; 2% paraformaldehyde, 0.1 M L-lysine, 0.01 M metaperiodate) in phosphate-buffered saline (0.1 M PBS, pH 7.4) for immunocytochemistry experiments, or lysed in guanidium-thiocyanate for total RNA isolation. As reported by Feron *et al.* (16) three types of cells, SUS, HBC and ORNs, were identifiable after 2–3 days of culture. After 6 days of culture, ORNs could no longer be detected (16; our own unpublished data).

Immunocytochemistry (ICC)

ICC assays were performed on either olfactory mucosa sections or OE cells in culture. Tissue sections were prepared as previously described (10). OE cells were fixed in PLP, as described above. For both OM sections and OE cells, nonspecific staining was blocked by incubation for 1 h at room temperature with non-immune serum appropriate to the secondary antibody at a dilution 1 : 10 in PBS containing 2% bovine serum albumin (BSA) and 0.2% Triton X-100. The OM sections and OE cells were then incubated overnight at 4 °C with primary antibody in PBS containing 0.2% BSA and 0.05% saponin. The following antibodies were used to identify different cell types in the olfactory epithelium: anti-β-tubulin III for neurones (1 : 800); anti-CK14 for horizontal cells (1 : 20; 15); anti-CK18 for sustentacular cells (1 : 50; 15). Antibodies against IR (ab10991 or SC 711), IRS-1, IRS-2, Pdx1 and insulin were used at the following dilutions: 1 : 500, 1 : 50, 1 : 100, 1 : 100, 1 : 1000 and 1 : 1000, respectively. For insulin ICC, OM sections were submitted to a demasking step at 94 °C in citrate buffer. Controls included the incubation of non-immune serum or nonspecific IgG in place of each primary antibody. Controls for IR and insulin also included preincubation of the IR antibody with 250 μg of rat liver plasma membranes (see preparation of membranes in *Insulin radio-receptor assay* section) and of the insulin antibody with 10 μg bovine insulin, for 1 h at room temperature. After centrifugation, the supernatant was incubated with OM sections or OE cells under the same conditions as the first antibodies. After washes in PBS, labelling was visualised using secondary antibodies conjugated either with fluorochrome (1 : 500, 1 h at room temperature) or biotin revealed by avidin-peroxidase kit with diaminobenzidine (DAB 0.5 mg/ml) and H_2O_2 (0.005%). Some sections or cells that had undergone ICC for IR, insulin and Pdx1 were then processed for a double-labelling after a 30-min blocking step in non-immune goat serum (1 : 10 in PBS, 2% BSA, 0.05% saponin) followed by incubation with CK14, CK18 or β-tubulin III antibodies as mentioned above. For immunofluorescence detection, preparations were washed in PBS and mounted in Vectashield (AbCys, Paris, France). For DAB detection, sections were air dried, dehydrated in ethanol, cleared in xylene and mounted in DePex (GURR; Labonord, Villeneuve d'Ascq, France). Images were acquired on either a DMBR Leica microscope equipped with an Olympus DP-50 CCD camera using Cell^F software (Olympus Soft Imaging Solutions GmbH, OSIS, Münster, Germany) or a Zeiss LSM 510 confocal microscope equipped with an ion-Argon (458 nm/488 nm/514 nm) and a Helium-Neon (543 nm) laser Carl ZeissAG, Oberkochen, Germany). They were processed using Cell^F, Image J (free Java port of NIH image, http://rsbweb.nih.gov/ij/) or Photoshop 7.0 (Adobe Systems Inc., San Jose, CA, USA) softwares. Images were adjusted for contrast and brightness to equilibrate light levels. Same levels of adjustment were used for the zero primary control as for those with primary antibody. Image content was not altered in any case. Confocal observations were made at the Mima2 facilities in Jouy-en-Josas (France).

Insulin extraction

After deep pentobarbital anaesthesia, the rats were sacrificed by decapitation. The OM was dissected, weighted and subjected to mild enzymatic digestion with RDB (30 min at 37 °C in Jocklic medium) to eliminate as far as possible any blood trapped in the tissue. After two washes with Joklic medium, tissue fragments were centrifuged (1500 *g* for 10 min), and the pellet was frozen in liquid nitrogen and stored at −80 °C until extraction. Insulin extraction was performed on fragments corresponding to each OM, using an acid-alcohol extraction protocol. At the end of the procedure, supernatants were lyophilised and reconstituted in 110 μl RIA buffer (Rat insulin RIA kit; Linco Research). An aliquot (10 μl) was taken for a Peterson protein assay (17). Rat pancreas (tissue control) and 1-ml aliquots of HCL/ethanol mix (blank control) were extracted under the same conditions. To evaluate insulin losses during extraction, 2 ng/ml rat insulin aliquots were extracted under the same conditions and evaluated in RIA. Mean recovery was 60%. A similar efficiency of insulin extraction was obtained by adding ^{125}I-insulin directly after OM homogenisation.

RIA

The insulin concentration in OM extracts and plasma was determined using the sensitive insulin RIA kit (Linco Research). The limit of sensitivity of the assay was 0.02 ng/ml. Inter and intra-assay coefficients of variation were 11% and 6%, respectively. We checked that blank control did not displace ^{125}I-insulin. Dilutions of olfactory mucosa extracts paralleled those of rat insulin. Insulin extracts were normalised to fresh tissue weight.

Western blotting

Olfactory mucosa tissues were homogenised in a cold buffer (10 mM Hepes-NaOH, 150 mM NaCl, 1 mM ethyleneglycol tetraacetic acid) containing 1% Nonidet-P-40, 1% phenyl-methylsulphonyl fluoride (PMSF) and a cocktail of anti-proteases (Complete; Roche Diagnostics). Samples were centrifuged for 30 min at 12 000 *g*, the supernatants were collected and protein levels quantified using the Peterson method. Whole OM extract dilutions or liver membranes (60 μg) as control, prepared as described in radio receptor assay section (see below) were loaded onto a 8% SDS-PAGE. Following electrotransfer, membranes were blocked with 4.5% nonfat milk and then incubated with the sc-711 IR antibody (1 : 500, overnight at 4 °C). After extensive washing in PBS-0.5% milk (4 × 15 min each), the membranes were incubated with horseradish peroxidase-conjugated anti-rabbit secondary antibody (1 : 5000; Sigma Aldrich). The targeted proteins were detected using an ECL western blotting detection kit (Amersham Biosciences, Orsay, France).

Reverse transcription-polymerase chain reaction (RT-PCR)

The presence of mRNAs coding for IR, IRS-1, IRS-2, insulin, Pdx1, PC1/3 and PC2 was assessed by RT-PCR on total RNAs extracts from OM (n = 3) or from OE cells in culture (n = 3). As controls, RT-PCR was performed on total RNAs of rat hypothalamus, liver, kidney and olfactory bulb. Rat pancreas total RNAs, either purchased from BioChain (Hayward, CA, USA), or kindly supplied by Dr R. Scharfmann, were also used as a control. Total RNAs were extracted using the guanidium-thiocyanate-phenol-chloroform extraction method. The purity and integrity of the RNAs were checked before carrying out the analytical procedures. RT on 4 μg of total RNA was followed by PCR performed as previously described (10). GAPDH gene expression was run as a quality control test for all cDNA samples. The primer sets used are described in Table 1. One microliter of cDNA was amplified in a 20-μl final volume PCR, consisting of denaturation at 94 °C (45 s), annealing (45 s) at appropriate temperatures for each primer set as mentioned in Table 1 and extension at 72 °C (45 s), for 40 cycles (IR-A and IR-B, Pdx1), 25 cycles (GAPDH) and 35 cycles (IRS-1, IRS-2, PC 1/3, PC2, preproinsulin I, preproinsulin II). For preproinsulins and Pdx1 amplifications, a second run of PCR was performed (nested PCR). One microliter of preproinsulin I and II and of Pdx1 first PCR products (diluted 1 : 100) was used for a second run of amplification using internal primer sets (preproinsulin-i and Pdx1-i, Table 1) for 35 additional cycles. PCR products were resolved on 1.5–3% agarose gel, sequenced (Genome Express, Paris, France) then analysed using BLAST programmes.

Real time PCR (qPCR)

To quantify IRs and preproinsulin transcripts in OM collected on normally fed (n = 5) or fasted for 48 h (n = 5) adult rats, 60 ng of cDNA obtained by reverse transcription was mixed with 10 μl Power SYBR Green PCR Master Mix (Applied Biosystems, Foster City, CA, USA) and 300 nM of each primer complementary to either IR, insulin or β-actin (chosen as the reference gene) in a 20-μl total volume (Table 2). The reaction mixture was finally transferred into a 96-well optical reaction plate, sealed with appropriate optical caps and run on the ABI Prism 7900HT apparatus (Applied Biosystems) under standard conditions. Each sample was run in triplicate and standard controls of both the specificity and efficiency of the qPCR assays were performed. Data were expressed as ΔCt, corresponding to threshold cycle (Ct) values normalised to the β-actin one in the same individual sample.

Table 1. Primers for Reverse Transcriptase-Polymerase Chain Reaction (RT-PCR) and Nested RT-PCR.

Gene product	Primers (5′ to 3′)	Amplicon size (bp)	Annealing °C	References
PCR				
IR				
Forward	TTCATTCAGGAAGACCTTCGAG	IR-A 223	58	(57)
Reverse	CAGGCCAGAGATGACAAGTGAC	IR-B 259		
IRS1				
Forward	GCCAATCTTCATCCAGTTGC	337	58	(57)
Reverse	CATCGTGAAGAAGGCATAGG			
IRS2				
Forward	AGCTGGTGGTAGTCATACCC	391	58	(57)
Reverse	CAGGTTCATATAGTCAGA			
PC1/3				
Forward	TGGAACCAGCACCGTACTGTTGG	132	55	(58)
Reverse	TCCACTCCTCTCCTGTCATTCTGGA			
PC2				
Forward	CAGCTTCACGATGAGGTTCA	226	53	(59)
Reverse	CCTCACATGCATTTGTTTGG			
GAPDH				
Forward	AAGGCTGAGAATGGGAAGCTG	564	58	(10)
Reverse	AAGCGGCATGTCAGATCCACA			
Nested PCR				
PreproINS I-e				
Forward	GCTACAATCATAGACCAT	392	56	(60)
Reverse	GGCGGGGAGTGGTGGACTC			
PreproINS II-e				
Forward	GCTACAGTCGGAAACCATC	381	56	
Reverse	ACAGGGTAGTGGTGGGCCT			
PreproINS-i				
Forward	ATGGCCCTGTGGATGCGCTT	330	60	
Reverse	GTTGCAGTAGTTCTCCAG			
Pdx1-e				
Forward	TACGCGGCCACACAGCTCTACAAGGAC	582	56	(61)
Reverse	CCACTTCATGCGACGGTTTTGGAACCAGA			
Pdx1-i				
Forward	CTCGCTGGGAACGCTGGAACA	225	56	
Reverse	GCTTTGGTGGATTTCATCCACGG			

Table 2. Primers for Quantitative Reverse Transcriptase-Polymerase Chain Reaction.

Gene product	Primers (5′ to 3′)	Amplicon size (bp)
IR-A		
Forward	CAGGCCATCCCGAAAGC	60
Reverse	GGTGTAGTGGCTGTCACATTGC	
IR-B		
Forward	TTACCTGCACAACGTGGTTTTT	58
Reverse	CTCAGCACCATTGCCTGAAG	
PreproINS1		
Forward	GCCCAGGCTTTTGTCAAACA	71
Reverse	TCCCCACACACCAGGTACAGA	
PreproINS2		
Forward	GGCTTTTGTCAAACAGCACCTT	66
Reverse	TCCCCACACACCAGGTAGAGA	
β-actin		
Forward	GACCCAGATCATGTTTGAGACCTT	61
Reverse	CACAGCCTGGATGGCTACGT	

Insulin radio-receptor assay (RRA)

OM, liver and olfactory bulb membranes (as controls) were prepared as followed: tissues were collected on fed (n = 4) or fasted for 48 h (n = 4) adult rats and homogenised in a Teflon glass homogeniser with a four-fold volume of 1 mM $NaHCO_3$ buffer containing 20% sucrose, 1 mM ethylenediaminetetracetic acid, 1 mM PMSF and 10 μg/ml leupeptin maintained at 4 °C. Homogenates were centrifuged at 9000 *g* for 30 min at 4 °C and resulting supernatants were further centrifuged at 105 000 *g* for 60 min at 4 °C. Pellets were suspended in the insulin binding assay buffer (see insulin binding assay section; 1 ml of buffer/g of homogenised fresh tissue) and stored at −80 °C. Protein concentration in membranes suspensions was determined using the method of Peterson.

Binding of ^{125}I-labelled insulin (^{125}I Tyr A14 porcine IR grade, specific activity 371 μCi/μg; NEN, Boston, MA, USA) to OM, liver and olfactory bulb membranes was performed in duplicate. Incubations were carried out overnight at 4 °C. The incubation volume of 250 μl in binding assay buffer (118 mM NaCl, 5 mM KCl, 1.2 mM $MgSO_4$, 10 mM Na_2HPO_4, 1% BSA, pH = 7.8) consisted of 50 μl of ^{125}I-insulin (30 000 c.p.m., 15 fmole/tube), 100 μl of membrane suspension (300 μg for liver and olfactory bulb or 500 μg of proteins for OM) and 100 μl of serial dilutions (0–1 μg/tube) of unlabelled bovine insulin (Sigma Aldrich) or human recombinant insulin growth factor (IGF)-1 (as specificity control; Chiron, Emeryville, CA, USA). At the end of the incubation period, 1 ml of cold assay buffer was added and samples were centrifuged at 12 000 *g* for 30 min at 4 °C. Pellets were washed with 200 μl of 10% sucrose. The radioactivity of the pellet was determined in a gamma counter (LKB 1272 clini gamma, LKB Instruments, Victoria, Australia). Specific binding (B0) was determined as the difference between total and nonspecific binding in the absence or presence (8 μg) of insulin. Scatchard plots were analysed with the LIGAND programme (G. A. Mcpherson, Biosoft, Cambridge, UK) by two sites noncomparative models.

Electro-olfactogramme (EOG)

EOG experiments were performed on hemi-heads prepared from six male rats aged 1–3 weeks and killed by decapitation. EOG recordings were made from rat OE in an opened nasal cavity configuration. The head was rapidly cut longitudinally and the nasal septum was removed to expose the endoturbinates. Experiments were performed at room temperature on both hemi-heads. One hemi-head was kept in a humid chamber for later use, whereas the experiment was performed on the other.

For recordings, the hemi-head was placed in a recording chamber on a custom-designed platform (Siskiyou, Inc., Grants Pass, OR, USA) of an upright Olympus BX51WI microscope (Olympus, Rungis, France) equipped with a low magnification objective (× 4) and MPC-325 motorised micromanipulators (Sutter Instruments, Novato, CA, USA). The odour stimulation device was modified from a previously described apparatus (18). Briefly, the hemi-head was kept under a constant flow of humidified filtered air (approximately 70 l/h) delivered close to the endoturbinates through a 9-mm glass tube. This tube was positioned 2 cm from the epithelial surface and was centred on the recorded endoturbinates. This preparation enabled the recording of stable signals for more than 3 h. Odour stimulations were performed by blowing air puffs (100 ms, 20 l/h) through an exchangeable Pasteur pipette enclosed in the glass tube and containing a filter paper impregnated with 20 μl of a given odorant (one odorant-one pipette). To prevent any air saturation with the odorant, an air flush was applied to the Pasteur pipette before it was placed in the glass tube and before subsequent odorant application.

EOG voltage signals were recorded using an Multiclamp 700B patch-clamp amplifier (Axon Instruments, Molecular Devices, Union City, CA, USA) used in a DC current-clamp configuration (I = 0), low-pass bessel filtered at 1 kHz and digitised at a rate of 2 kHz using an Digidata 1322a A/D converter (Axon Instruments) interfaced to a Pentium PC and Pclamp 9.2 software (Axon Instruments). A reference Ag/AgCl electrode was placed on the frontal bone overlaying the olfactory bulb. Recordings were made with glass micropipettes of 4–5 MΩ filled with a mucosal saline solution (45 mM KCl, 20 mM $KC_2H_3O_2$, 55 mM $NaCH_3SO_4$, 1 mM $MgSO_4$, 5 mM $CaCl_2$, 10 mM HEPES, 11 mM glucose, 50 mM mannitol, pH 7.4, 350 mOsm adjusted with mannitol). The composition of this solution was chosen to match the composition of mucus as closely as possible, according to previous studies (19). The recording electrode was placed in the centre of endoturbinates II′ and III. This position provided robust, reproducible and long-lasting EOG recordings in the range 6–19 mV in response to isoamyl acetate and citral (1 : 10 pure odorant diluted in dimethyl sulphoxide). Odour stimulation with dimethyl sulphoxide alone always produced a signal of < 1 mV amplitude.

One drop of approximately 0.1 μl of mucosal saline solution alone or with 1 μM bovine insulin was delivered by capillarity onto the recorded area of endoturbinates II′ or III using another glass micropipette (approximately 5 μm in diameter). This drop covered approximately 1 mm of the diameter of the olfactory epithelium and was checked under the microscope. Insulin treatment (0.5–1 ng by endoturbinates) alternated between the two endoturbinates (II′ and III) of the different hemi-heads. Responses to both odorants were then recorded every 5 min on each endoturbinate. Analysis were performed off-line using Clampfit 9.2 (Axon Instruments). Peak amplitude and onset slope (from 10% to 90%) were measured. EOG responses decay was fitted with a double exponential function, showing fast and slow components. Fast decay (from 100% to 50%) and slow decay (from 40% to 10%) slopes were respectively measured and normalised to the response prior to local treatment.

Statistical analysis

Data presented in the text and figures are expressed as mean ± SEM. For qPCR and binding analysis, statistical comparisons were performed using the nonparametric Mann–Whitney test. To analyse EOG data, we first used a two-way analysis of variance (ANOVA) to determine the overall significance of the time and insulin treatment effects. When the ANOVA indicated a significant effect, post-hoc Tukey or Bonferroni multiple comparison of means test were used to determine individual differences between responses at each time considered, and differences over time for each treatment. $P < 0.05$ was considered statistically significant.

Results

Expression and cellular distribution of insulin receptor in the olfactory mucosa

Both insulin receptor transcripts are present in the OM

Total RNAs prepared from OM and from liver (with hypothalamus and olfactory bulb as controls) were reverse transcribed and analysed by PCR using oligonucleotide primers flanking exon 11 of the IR sequence to amplify long (IR-B) or short (IR-A) isoforms. As previously described (20), liver preferentially expressed the long form of the IR, and hypothalamus and bulb expressed the short form, and the amplified transcripts revealed the expected size. We found that both isotypes were expressed in the OM (Fig. 2A). OE cells in culture expressed IR-A and -B at 50 h; both transcripts were still detected after 10 days of culture (Fig. 2B). Real-time PCR (primer sets in Table 2), as used to evaluate the respective level of expression of both IR transcripts in the OM, showed that IR-A and -B were equally present. Expression levels in the OM of both IR-A and IR-B were similar to their respective controls: the olfactory bulb for IR-A (ΔCt: OM = 7.79 $\pm$ 0.18, n = 3; olfactory bulb = 8.38 $\pm$ 0.19, n = 3) and the liver for IR-B. (ΔCt: OM = 8.81 $\pm$ 0.81, n = 3; liver = 7.61 $\pm$ 0.58, n = 3).

Insulin receptors are expressed in the OM and localised in neuronal and non-neuronal cells

Western blot analysis of OM protein extract and liver membranes (as a control), using antibody against IRβ-subunit (sc-711), showed the same major band of the expected size for IRβ (97 kDa; Fig. 2C).

OM sections were subjected to immunohistochemical analysis with a second type of antibody against the IR β-chain (ab 10991). Tissue section analysed with IR β-chain revealed with fluorescent secondary antibody (Fig. 3A), showed a strong IR immunoreactivity in the EO at the apical pole, corresponding to SUS cells and mature neurones, and at the basal pole corresponding to GBC and HBC basal cells. Immature neurone somata in the medium part of the OE were very faintly labelled. We also detected a signal in the lamina propria in the endothelium of blood vessels. The signal detected in Bowman's glands (yellow arrow) resulted in part from background because it was also observed in control sections incubated with non-immune rabbit serum (Fig. 3B, yellow arrow). A second set of tissue sections incubated with the second IR β-chain antibody (sc-711) and revealed with DAB secondary antibody showed more acute IR labelling on mature ORNs (ORNm), especially on their knobs (Fig. 3D), on immature ORNs (ORNi; Fig. 3E) and on SUS and basal cells (Fig. 3F).

Primary cultures of OE cells were used to confirm the cellular localisation of IR by double-labelling. After 50 h of culture, all cell types initially present in the epithelium could be easily characterised. Non-neuronal and neuronal cells were labelled by IR β-chain antibody (ab 10991; Fig. 3G). The strongest labelling was present on the neurites of neurones (Fig. 3G arrow). Double-labelling with β-tubulin III confirmed that approximately 70% of neurones expressed IR with a high density signal on their neurites (Fig. 3H). Some neurones did not display a double-labelling signal, thus revealing an absence of IR expression (Fig. 3I). SUS cells identified by CK18 (Fig. 3J) and HBC cells identified by CK14 (Fig. 3K) also exhibited IR labelling. No signal was observed in cells incubated with IR antibody pre-incubated with liver membranes (Fig. 3L) or cells incubated with non-immune rabbit and mice serum at the same concentrations as IR, CK or β-tubulin III antibodies

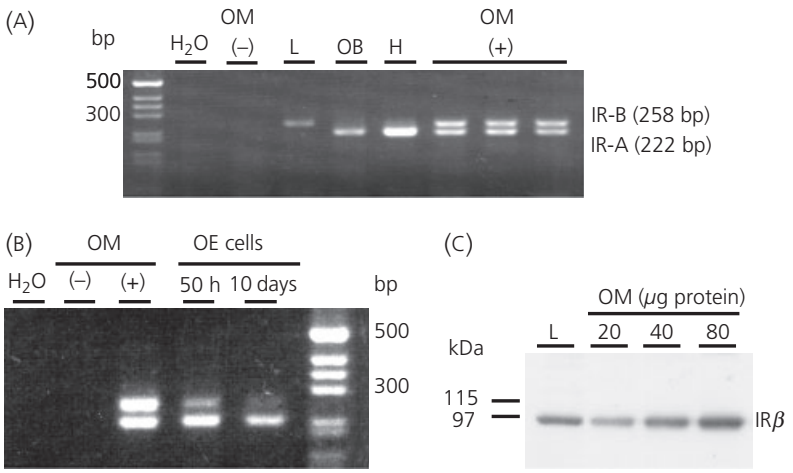

Fig. 2. Expression of both insulin receptor transcripts in the olfactory mucosa (OM). (A) reverse transcriptase-polymerase chain reaction (RT-PCR) analysis of insulin receptor (IR)-A and IR-B in OM; PCR products for full-length (IR-B, 258 bp) and truncated (IR-A, 222 bp) mRNAs were detected on a 3% agarose gel stained with ethidium bromide. Control lanes were loaded with amplified cDNA derived from the liver (L), hypothalamus (H) and olfactory bulb (OB) as controls. The liver expressed IR-B and hypothalamus and olfactory bulb expressed IR-A mRNAs. Both IR-A and IR-B were observed in OM. (B) RT-PCR analysis of both IR isoforms in olfactory epithelium cells in culture. IR-A and IR-B were detected after 50 h of culture (neuronal and non-neuronal cells) and 10 days of culture (non-neuronal cells). (C) IR protein is expressed in OM. Different amounts of total OM protein extracts were separated by SDS-PAGE, transferred onto nitrocellulose membranes and probed with IRβ (sc-711) antibody. Liver membranes (L, 60 μg) were used as controls.

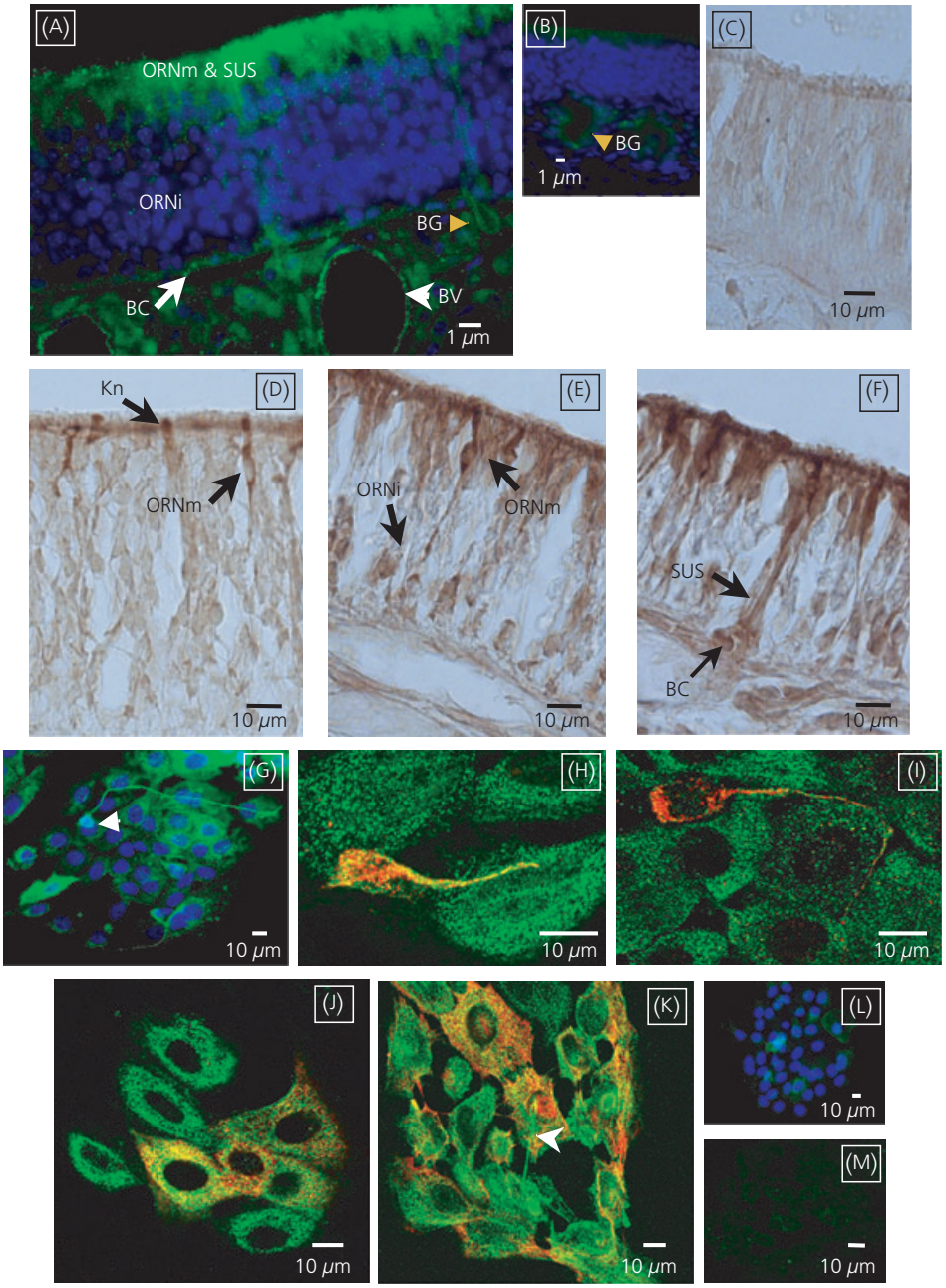

Fig. 3. Localisation of insulin receptor in olfactory mucosa (OM) and olfactory epithelium (OE) cells. (A) Insulin receptor (IR) localisation in OM section (light microscope, Alexa 488 detection). Stronger signal was detected in the upper part of the OE corresponding to sustentacular cells (SUS) and mature olfactory receptor neurones (ORNm), in basal cells (BC, white arrow) and in the endothelium of blood vessels located in the lamina propria (white arrow head). Lower signal was observed in immature ORNs (ORNi). The signal detected in Bowman's glands (yellow arrow) resulted in part from the background as it was also observed in control sections (B; yellow arrow), incubated with non-immune rabbit serum. (C–F). More acute IR detection in OE sections, revealed with DAB, confirmed IR localisation in ORNm (D, E) and ORNi (D), in the dendritic knobs of ORNm (Kn, E) and in the SUS and BC (F). No signal was observed in control sections incubated with non-immune rabbit serum (C). (G, H, I, L) IR detection in OE cells after 50 h of culture (light microscope). Non-neuronal and neuronal cells were labelled (G). An intense signal was observed in neuronal neuritis (G, white arrow head). No signal was observed in control cells incubated with IR antibody pre-incubated with liver membranes (L). (H, I, J, K, M) OE cells were double-labelled with IR antibody (Alexa 488 detection, green signal) and different antibodies (β-tubulin III, and CKs; Alexa 555 detection, red signal) to identify them. OE cells expressing IR were characterised by double-labelling (merged yellow signal) and analysed with a confocal microscope. Neurones identified by β-tubulin III expressed IR particularly in their neuritis (H); some neurones (red) did not express IR (I). IR expression was also observed in SUS cells identified by CK 18 (J) and horizontal basal cells identified by CK 14 (K; white arrow indicates IR green labelling of a neurone laying on these cells). No signal was observed in double-labelled control cells incubated with non-immune rabbit and mice serum at the same concentrations as IR, CK or β-tubulin III antibodies (M).

(double-labelling control; Fig. 3M). Unfortunately, we did not succeed in identifying GBC cells using Dr J. E. Schwob's GBC antibody, because of a strong aspecific signal.

Insulin binding on olfactory mucosa membranes (Fig. 4)

Membranes from OM bound ^{125}I-insulin. At a final membrane concentration of 2 mg/ml, 5% of the ^{125}I-insulin was specifically bound. Half-maximal displacement of tracer insulin (IC_{50}) was obtained with an insulin concentration of 0.5 nM. Recombinant IGF-1 was 100-fold less potent in competing for ^{125}I-insulin (Fig. 4A). Data analysed by Scatchard plot (Fig. 4B) suggested a two-orders receptor sites model: a high affinity site with an affinity constant of $1 \pm 0.2\ 10^9$/M and a binding capacity (B_{max}) of 18 ± 9 fmol/mg and a low affinity site with an affinity constant of $0.06 \pm 0.01\ 10^9$/M and a B_{max} of 122 ± 23 fmol/mg (n = 4). As a comparison, binding characteristics of membranes prepared from livers and olfactory bulbs collected on the same animals were: liver, high affinity site, affinity constant of $1.9 \pm 1.5\ 10^9$/M and B_{max} of 153 ± 90 fmol/mg and low affinity site, affinity constant of $0.09 \pm 0.05\ 10^9$/M and B_{max} of 2.8 ± 1.4 pmol/mg; olfactory bulb, high affinity site, affinity constant of $3 \pm 0.58\ 10^9$/M and B_{max} of 69.53 ± 10.86 fmol/mg and low affinity site, affinity constant of $0.26 \pm 0.2\ 10^9$/M and B_{max} of 0.7 ± 0.2 pmol/mg (data not shown).

IRS-1 and -2 are expressed in the OM (Fig. 5)

Among the proteins phosphorylated after insulin binding to its receptors, IRS-1 and IRS-2 are considered as major mediators in metabolic functions and are strongly expressed in the brain (21, 22). The expression of both IRS transcripts was detected in OM (Fig. 5A, B). Transcripts were of the same size as those detected in total RNAs prepared from hypothalamus (IRS1) and kidney (IRS2) used as controls. OM sections were subjected to ICC analysis with antibodies against IRS-1 and IRS-2 (Fig. 5C). IRS-1 and IRS-2 were found to be widely expressed in OM cells. No signal was observed on control sections incubated with non-immune rabbit serum.

Local production of insulin in the olfactory mucosa

A possible local production of insulin was verified by testing the presence of transcripts for preproinsulin I and II and for factors related to insulin production, such as Pdx1 and PC1/3 and PC2. The immunodetection of insulin and Pdx1 was also performed on OM sections or OE cells after 50 h of culture.

Preproinsulin I and II, Pdx1, PC1/3 and PC2 transcripts are present in the olfactory mucosa

Total RNA prepared from the pancreas (as a control), OM or OE cells after 50 h and 10 days of culture were reverse transcribed and analysed by PCR using the first set of preproinsulin I and II primers (Table 1). Direct PCR amplification of both preproinsulin transcripts was only observed with the control pancreas sample (Fig. 6A, two upper panels). Nested PCR using the preproinsulin internal nested primer set (Table 1) enabled the detection of both preproinsulin transcripts in OM and OE cells after 50 h and 10 days of culture (Fig. 6A, two lower panels). Using real-time PCR (primer set in Table 2), preproinsulin I and II transcripts were found to be equally expressed in the OM. However, the two transcripts were expressed three million times less frequently in the OM than in the pancreas.

Pdx1 transcript amplification was only observed in OM after a nested PCR, whereas, in the pancreas, amplification products were detected after the first PCR (Fig. 6B, left panel). PC1/3 (Fig. 6B, middle panel) and PC2 (Fig. 6B, right panel) transcripts were detected in the OM and in the pancreas after one amplification run.

Immunodetection of insulin in olfactory mucosa (Fig. 6C)

Insulin labelling was detected in the OE and in lateral nasal glands (Fig. 6Ca). In the OE, the signal was mainly localised at the apical (Fig. 6Cc, arrow 1) and basal pole (Fig. 6Cc, arrow 2). The localisation of this signal, compared with the CK18 labelling (Fig. 6Ce, arrows 1 and 2), strongly suggested that SUS cells expressed insulin. The labelling in basal layer corresponded to insulin localisation in the end feet of SUS cells because it was observed in an area without

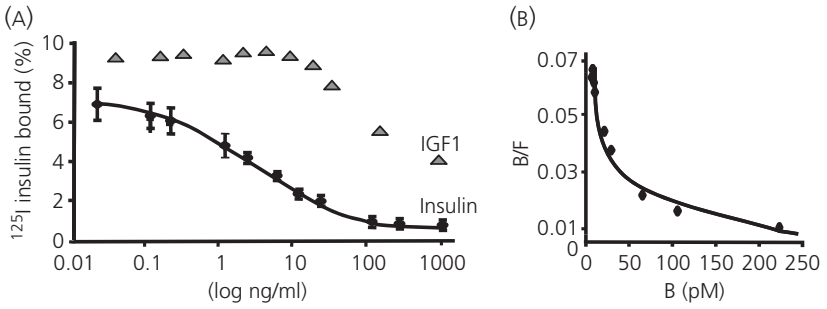

Fig. 4. Insulin binding on olfactory mucosa membranes. (A) Displacement of ^{125}I-insulin bound on olfactory mucosa (OM) membranes isolated from four individual normally fed rats. The membranes (2 mg protein/ml) were incubated with 0.1 nM of ^{125}I-insulin in the presence of unlabelled insulin or insulin growth factor-1 over a range of concentration from 0–1000 ng/ml (Values are mean ± SEM, n = 4). (B) Scatchard plot analysis of insulin displacement curve indicated that the specific binding of this hormone on OM membranes fitted a two-orders binding sites model.

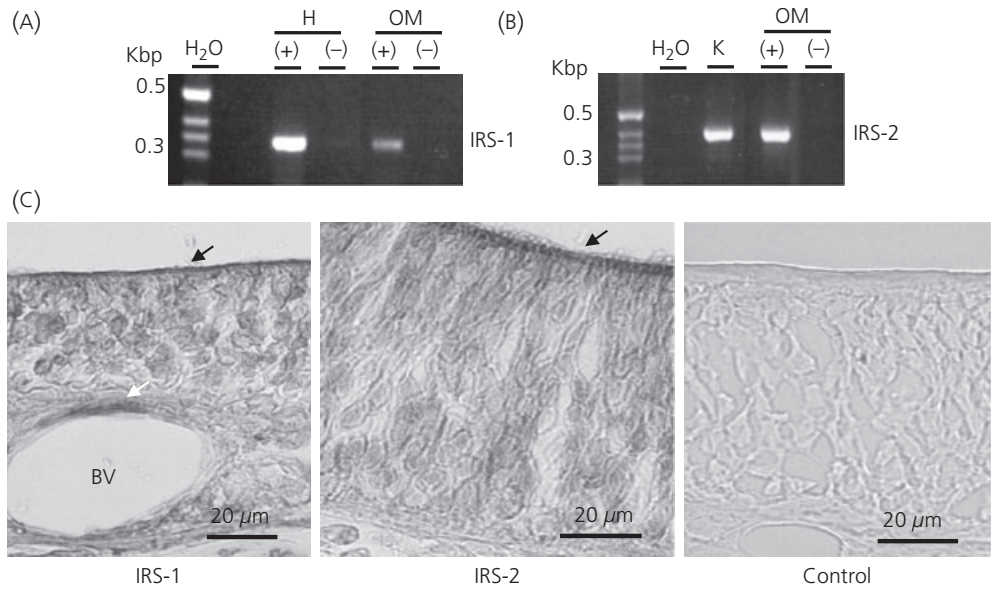

Fig. 5. Expression of insulin receptor substrate (IRS)1 and IRS2 transcripts and proteins in the olfactory mucosa (OM). (A, B) Reverse transcriptase-polymerase chain reaction (RT-PCR) analysis of IRS-1 (A) and IRS-2 (B) transcripts in OM; PCR products were detected on 3% agarose gel stained with ethidium bromide. Hypothalamus (H) PCR products were used as controls for IRS-1 and kidney (K) PCR products for IRS-2. (C) Immunodetection of both IRS in OM (light microscope). OM sections underwent immunohistochemistry analysis with antibodies against IRS-1 (left panel) or IRS-2 (middle panel). IRS-1 and 2 immunoreactivity was detected in all OM cells. The strongest signal was observed at the apical pole of olfactory epithelium (OE) (black arrow) and on the endothelium of lamina propria blood vessel (BV, white arrow). No staining was detected in section incubated with rabbit non-immune serum (right panel).

nucleus (Fig. 6cd, arrow 2′) and did not co-localised with CK14 labelling, identifying HBC (Fig. 6cd). Unfortunately, we did not succeed to co-localised insulin and CK18 signal. No signal was observed in the lamina propria, including the endothelium of blood vessels (Fig. 6cc, arrow 3) and Bowman's glands (data not shown). Control sections incubated with non-immune rabbit serum at the same concentrations or with insulin antibody pre-incubated with 10 μg bovine insulin (Fig. 6cb) were negative.

Immunodetection of Pdx1 in OE cells in culture (Fig. 7)

The cellular identity of cells likely to synthesise insulin, and therefore to express Pdx1, was verified on OE cells in culture by means of double-labelling using CKs or β-tubulin III antibodies. When detected, Pdx1 was localised in the nucleus of cells, as expected. It was found expressed in some SUS cells (Fig. 7). However, labelling was also observed in horizontal and neuronal cells (data not shown).

Insulin content in olfactory mucosa

The insulin content was evaluated in OM extracts by radioimmunoassay and compared with levels in the pancreas extracted under the same conditions. Mean insulin concentrations in the OM were 7.37 $\pm$ 0.48 pg/100 mg of fresh tissue (n = 7 independent OM; mean weight of one dissected OM: 100 mg). This concentration was far lower than in the pancreas (1.15 $\pm$ 0.2 μg/100 mg; n = 3).

Modulation of insulin-receptor in the OM after 48 h fasting

Insulin blood levels in fed and fasted animals

As expected, insulin plasma levels were decreased in fasted rats compared to fed ones (0.3 $\pm$ 0.1 versus 4.6 $\pm$ 1.1 ng/ml respectively, $P < 0.01$, n = 5).

Fasting has no effect on IR and insulin transcripts expression in the OM

Real-time RT-PCR was used to quantify and compare IR and insulin transcripts expression in fed and fasted rats OM. Expression levels of both IR isoform transcripts were not modified by fasting (ΔCt: fed IR-B = 11.23 $\pm$ 0.96 and IR-A = 10.9 $\pm$ 0.93; fasted IR-B = 11.68 $\pm$ 0.79 and IR-A = 11.32 $\pm$ 0.70; n = 4). Expression levels of both preproinsulin transcripts were similarly unchanged (ΔCt: fed preproinsulin I = 18.21 $\pm$ 1.21 and preproinsulin II = 17.15 $\pm$ 0.92; fasted preproinsulin I = 16.70 $\pm$ 1.11 and preproinsulin II = 15.93 $\pm$ 1.39).

Fasting increases IR number and insulin content in the OM (Fig. 8)

Compared with fed animals, fasted animals had a 55% increase of insulin binding (% of ^{125}I-insulin specific binding; fed = 5.6 $\pm$ 0.3; fasted = 8.7 $\pm$ 1%). Displacement curves (Fig. 8A) analysed by

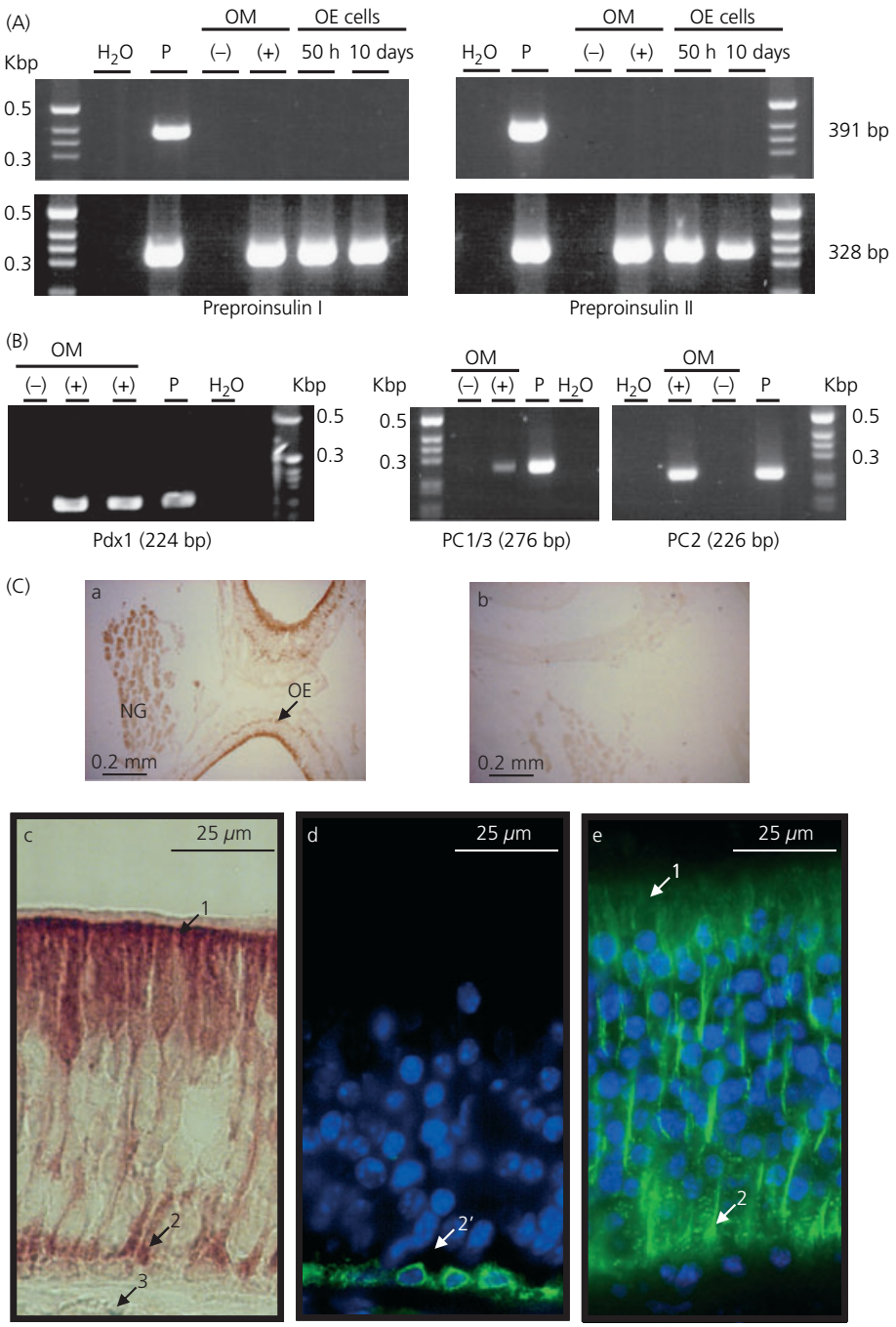

Fig. 6. Insulin expression in olfactory mucosa (OM). (A) Nested polymerase chain reaction (PCR) analysis of preproinsulin I (left panels) and II (right panels) transcripts in OM, and olfactory epithelium (OE) cells after 50 h (neuronal and non-neuronal cells) and 10 days of culture (non-neuronal cells). Upper panel: Preproinsulin I and II transcripts after direct PCR of pancreas (P) used as a control. Lower panel: Detection of both transcripts in OM and OE cells by nested PCR using a second set of primers. (B) Pdx1 transcript detection by nested PCR analysis in OM and pancreas (P) as a control (left panel); prohormone convertases PC1/3 and two transcripts detection by RT-PCR analysis in OM and pancreas (P) as a control (right panel). (C) Immunohistochemical localisation of insulin in the olfactory mucosa. Labelling (DAB detection) was present in the OE and in the lateral nasal glands (NG, panel a). In OE (panel c), signal was observed at the apical (arrow 1) and basal (arrow 2) parts of the epithelium. In the lamina propria, no labelling was observed even in blood vessels endothelium (arrow 3). No signal was detected in control section of OM labelled with insulin antibody pre-incubated with 10 μg insulin (panel b, DAB detection). Double-labelling of the same slide with CK14 antibody (panel d, horizontal cells identification, Alexa 488 detection) showed that insulin signal at the basal pole of the OE was not localised in the horizontal cells. In this last panel, arrow 2′ indicates an area without a nucleus where insulin labelling was observed in panel c, corresponding to SUS end feet. Localisation of insulin signal displayed the same distribution as CK 18 labelling (arrows 1 and 2), performed on a different slide (panel e, SUS identification, Alexa 488 detection).

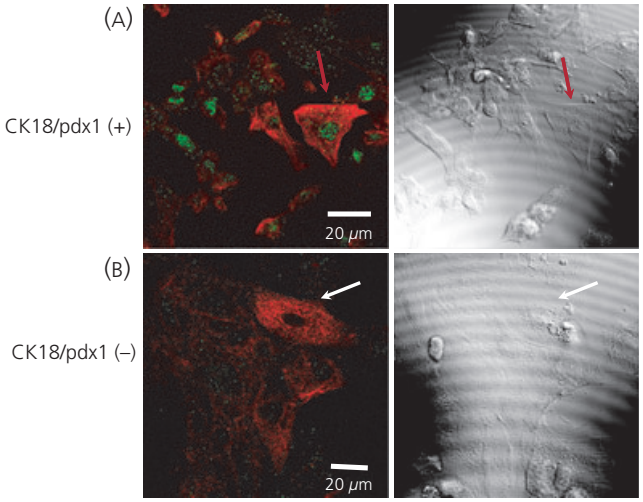

Fig. 7. Localisation of transcription factor Pdx1 in sustentacular cells after 50 h of culture (confocal images). (A) Pdx1 immunoreactivity (green signal) was present in the nucleus of sustentacular cells (SUS) (red arrow) identified by CK18 red labelling. (B) Some SUS did not express Pdx1 (white arrow). Right panels in grey correspond to transmission images.

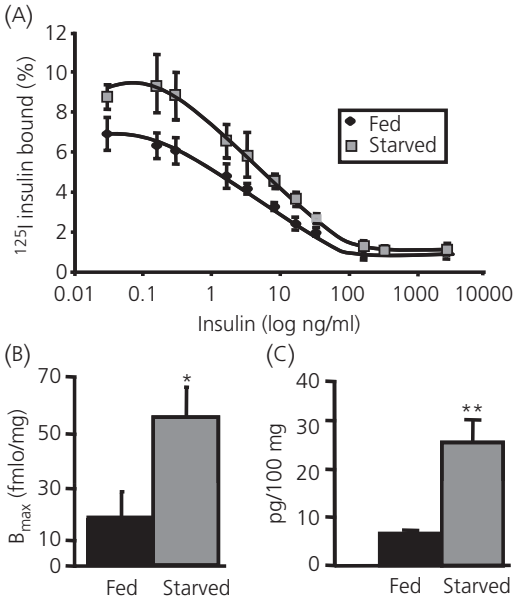

Fig. 8. Effect of 48 h starvation on insulin binding and insulin content in the olfactory mucosa. Each value represents the average of determinations from four (A, B) or five (C) independent olfactory mucosa (OM) respectively; Mean ± SEM. (A) Binding of 0.1 nM of ^{125}I-insulin to olfactory mucosa membranes (500 μg) of fed and starved animals was examined in the presence of 0–1.5 μM unlabelled insulin. Binding, expressed as percentage of total ^{125}I-insulin, was increased by starvation. (B) Binding capacity (B_{max}) of high affinity sites in OM membranes collected on starved animals was significantly increased (*$P < 0.05$). (C) Insulin concentration in extracts of OM collected in starved animals was higher than in extracts of OM collected in fed animals (**$P < 0.01$; Values are expressed as 100 mg of fresh tissue, which is the mean weight of one dissected OM).

Scatchard plot showed that starvation increased high affinity IR number (Fig. 7B), without affecting affinity constant (B_{max}: fed animals = 18 ± 9 fmol/mg versus starved animals = 55 ± 11 fmol/mg, n = 4, $P < 0.05$). Insulin content evaluated in OM extracts by radioimmunoassay was higher in starved animals than in fed one (26.3 ± 5 versus 6.9 ± 0.6 pg/100 mg fresh tissue, n = 5, $P < 0.01$, Fig. 8C).

Modulation of ORN response to odours (Fig. 9)

To determine a neuromodulating role for insulin on ORNs, we performed EOG on endoturbinates II′ and III treated simultaneously with mucosal saline solution, with or without 1 μM insulin (Fig. 9A). Responses to two odorants, isoamyl acetate and citral, were recorded for 30 min following treatment on both endoturbinates and normalised to the amplitude of the response prior to local treatment (Fig. 9B). Under control conditions, isoamyl acetate and citral applications evoked EOG responses with mean negative peak amplitudes of −12.20 ± 0.75 mV (n = 12) and −10.10 ± 1.17 mV (n = 12), respectively. Treatment with the mucosal saline solution for 30 min did not significantly change the amplitude of responses to the two odours (Fig. 9C), whereas local treatment with insulin (0.5–1 ng by endoturbinates) reversibly reduced their responses. This reduction was significant 5 and 10 min after the treatment. The inhibition of isoamyl acetate and citral evoked EOG responses peaked negatively after 10 min to 60.39 ± 11.50% of the control (n = 6, $P < 0.01$) and 73.00 ± 13.70% of the control (n = 6, $P < 0.05$; Fig. 9C) respectively. The amplitude of the response slowly returned to its initial value, 15–30 min later. The recorded EOG responses displayed a usually described rapid rising phase and a slower decay phase comprising fast and slow components (Fig. 9B). Because the EOG response kinetics was found to highly correlate with the amplitude across all experimental conditions, the onset and the two decay slopes were normalised to the corresponding response peak amplitude prior to statistical analysis. On average, isoamyl acetate and citral evoked EOG responses displayed normalised onset slopes of 9.17 ± 1.83/s and 7.82 ± 0.46/s respectively (n = 6), followed by normalised fast decay slopes of −0.53 ± 0.13/s and −0.77 ± 0.09/s respectively (n = 6), and normalised slow decay slopes of −0.17 ± 0.02/s and−0.10 ± 0.01/s respectively (n = 6). These kinetics were stable over time and were not significantly modified by mucosal solution local treatments (Fig. 9D). By contrast to its inhibitory effect on the EOG response amplitude, insulin did not significantly modify the kinetics of isoamyl acetate and citral evoked responses (n = 6; Fig. 9D).

Discussion

The present study provides the first demonstration of the presence of insulin receptors in the olfactory mucosa and of insulin involvement in the modulation of the responses of ORNs to odorants. Furthermore, we show that nutritional status modulates insulin receptor expression.

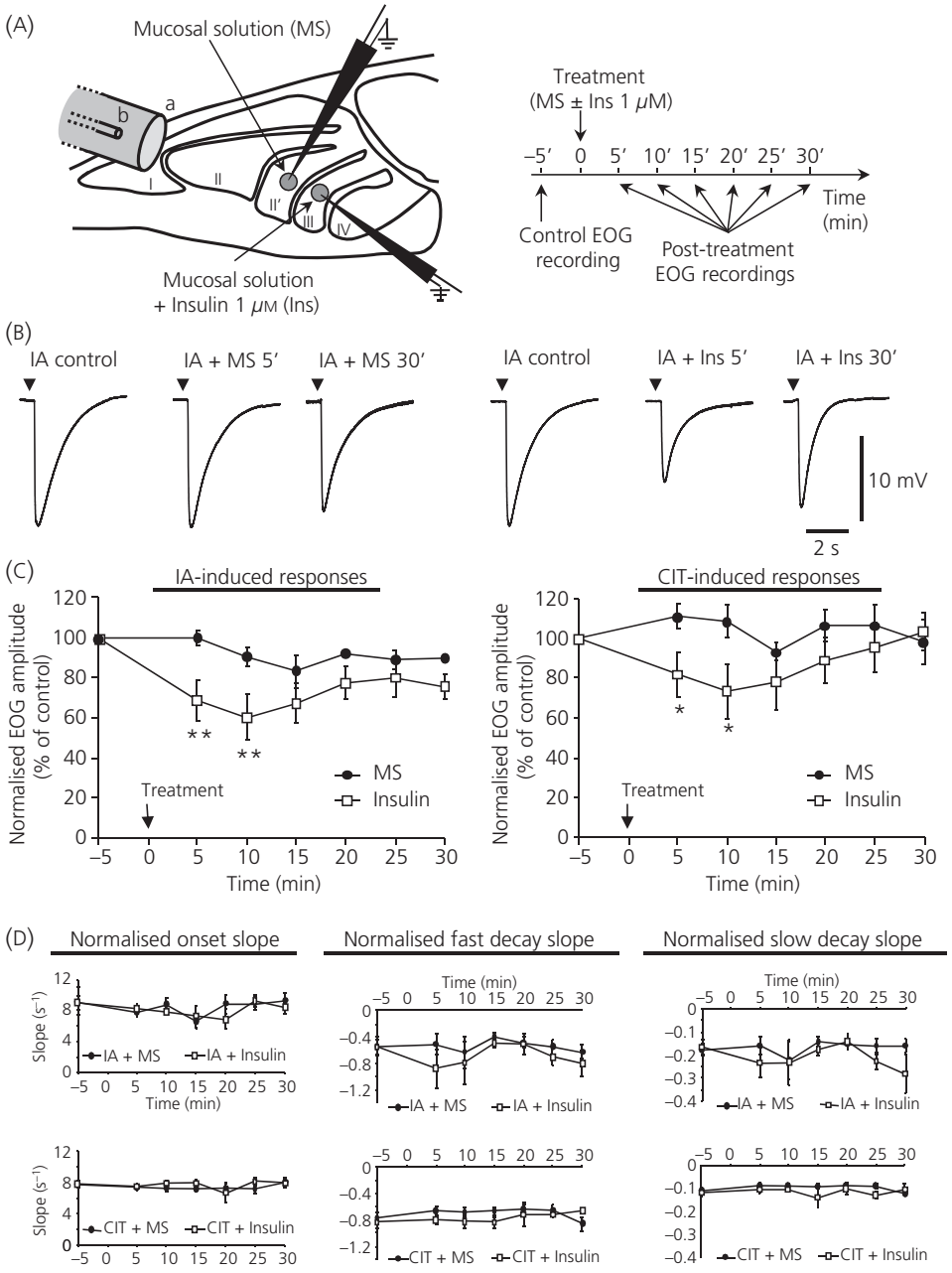

Fig. 9. Insulin reduces electro-olfactogramme (EOG) responses. (A) Schematic diagram of the experimental preparation. Turbinates were exposed in rat hemiheads; odorants (IA, isoamyl acetate; CIT, citral) were delivered rostrally through a Pasteur pipette (b) enclosed in a glass tube (a). The recording electrodes are represented on turbinates II′ and III. The time course of recordings and insulin treatment are described on the right. (B) Typical EOG responses to IA before and after treatment (0, 5 and 30 min) with 0.1 μl of mucosal solution (MS) alone (left) or containing 1 μM of insulin (right). (C) Effects of MS or MS + insulin (1 μM) treatments on the time course of EOG amplitudes in response to IA (left panel) and CIT (right panel). Mean ± SEM values (n = 6) are expressed as % of control EOG recordings prior to treatment (*P < 0.05; **P < 0.01). (D) Effects of MS or MS + insulin (1 μM) treatments on the time course of EOG kinetics in response to IA (upper panels) and CIT (lower panels). Onset slopes (left panels), fast decay slopes (middle panels) and slow decay slopes (right panels) are normalised to the corresponding EOG peak amplitudes and presented as mean ± SEM values (n = 6).

We found the presence in the OM of high levels of IR (transcripts and protein), in addition to transcripts encoding for proteins involved in the first step of the IR transduction cascade (IRS1 and IRS2). IR can be expressed in two variant forms, a short one (IR-A) and a long one (IR-B), both transducing insulin signals (13). We show that both isoforms are expressed in the OM at a comparable level. This was unexpected because OM is a neuroepithelium and IR-A is the predominant form expressed in brain tissues (13). The level of expression of both transcripts is quite high, with the IR-A level being comparable to that in olfactory bulb and the IR-B level comparable to that in liver. Insulin binding experiments on OM membranes also indicate a relatively high level of IR. Scatchard

transformation of the displacement curve fitted with a two sites model: a high affinity-low capacity site and a low affinity-high capacity site as described for the liver, olfactory bulb and many other tissues (23). Both affinity constants were comparable to those of the liver receptor. The number of high affinity sites in the OM was quite high compared to the liver and to the olfactory bulb, both displaying high specific insulin binding. In the OM and in OE cells in culture, IR protein was mostly expressed in sustentacular cells, horizontal cells and in neurones, showing an intense labelling of neuronal processes. A similar cellular localisation was found for the two major IRS proteins (IRS-1 and IRS-2). Those results support possible various roles of insulin in the OM.

As in other peripheral tissues, insulin in OM mainly originates from the peripheral circulation. How the hormone is transported from the blood remains to be investigated because the endothelium of the lamina propria vessels display tight junctions that partially isolate the OM from blood constituents (24). This transport may implicate the IR that we detected in the endothelium of the lamina propria vessels as already described for the blood–brain barrier in different regions of the brain (25). In addition to the peripheral insulin source, our data suggest the existence of a second source of insulin originating from the OM. Two different insulin genes encoding for preproinsulin I and II are reported in the rat (26). Extra-pancreatic expression of these genes has been described in various tissues (27). In the OM and its derived primary cell cultures, we detected these two transcripts expressed at comparable levels. The existence of the transcripts coding for the insulin transcription factor Pdx1 and for the prohormone convertases PC1/3 and 2, which are required for insulin maturation (28), reinforces the thesis of a local source of insulin. Indeed, RIA analysis of OM extracts confirmed the presence of the protein in this tissue. Its concentration was very low compared to peripheral circulating insulin level even in starved animals (200- and ten-fold less than circulating insulin concentrations in a satiated and 48 h starved animal, respectively). Similar low concentrations have already been reported in the rat brain (29) and olfactory bulb (8). Insulin protein was localised in sustentacular cells and in lateral nasal glands. This detection did not result from insulin binding to its receptors because no signal was observed in the endothelium of the lamina propria blood vessels where we detected insulin receptor. Consistent with the detection of insulin in sustentacular cells, we found Pdx1 expression in the nucleus of these cells in culture.Because plasma insulin levels are clearly related to nutritional status, we investigated whether fasting influenced IR expression and insulin concentration in the OM both at the mRNA and protein levels. Forty-eight hours of fasting, leading to insulin plasma level 15-fold less than in fed animals, induced an increase in insulin binding capacities in the OM, without any detectable change of the level of both IR transcripts. This increase was due to a higher IR number (high affinity sites) but not to an enhancement of their affinity for insulin. Such an inverse relationship between insulin circulating levels and IR expression was already reported for the liver (30). However, modulation of IR expression by the nutritional status appears to be differentially regulated at the two levels of olfactory message processing, the peripheral one (OM) and the central one (olfactory bulb). In the olfactory bulb, insulin binding was not affected by 48 h of fasting (31), although insulin content was increased (8); 4 days of complete fasting were necessary to induce a modification of insulin binding consisting of a decrease rather than an increase (32). Concerning insulin concentration in OM, we showed that it was increased after 48 h of fasting without any modification of both preproinsulin transcripts levels. Such an increase, when circulating insulin is decreased, reinforces the hypothesis of a local source of this hormone in the OM. However, enhanced IR expression could also lead to an increased insulin transport through the endothelium of lamina propria blood vessels, from the plasma to the OM.

Regardless of the local or endocrine origin of this insulin, what would be its physiological role? Because of the expression of both IR isoforms in neuronal and non-neuronal cells, different effects, already reported in other tissues, could be postulated. Insulin may be involved in the maintenance of glucose level in EO cells. Neuronal and non-neuronal cells may be targets for the regulation of the glucose transporter GLUT4 redistribution by insulin, as suggested in the hypothalamus (33). In these cells, insulin may also regulate glucokinase gene expression through IR-B signalling (34, 35). At the sustentacular cell level, insulin may activate the transcription of its own gene, signalling through its fixation on IR (35). However, one of the main roles of insulin in OM may concern cell survival because this tissue is continuously renewed throughout life. Indeed, the olfactory neurone population is subjected to constant neurogenesis and apoptosis (36, 37). Mitogenic and anti-apoptotic roles for insulin have been reported in different models (38) and this hormone is an important survival factor for OE cells in culture (39). In many tissues, this survival effect appears to act through IR-A signalling (38). Furthermore, previous studies reported the involvement of insulin/insuline-like growth factor I in neuroprotection (40, 41) and neurogenesis in the OB and the OE (42, 43).

Such essential roles for insulin in the OM would require the maintenance of a threshold level of the hormone in this tissue when a rapid decrease of its concentration occurs in the peripheral circulation. It seems to be the case after 48 h of fasting, when local insulin concentration is enhanced in the OM.

Very little is known about a peripheral modulation of odour detection related to feeding status. Previous studies had mainly focused on how the central nervous system adapts food intake as a function of nutritional status (44). However, some experiments have shown that part of this adaptation may also occur at the level of the peripheral sensory system. This holds particularly true for taste organs and has been well described in invertebrates (45) and in rodents where leptin modulates responses to sugars and fatty acids (46, 47). In the olfactory system, neuropeptide Y and endocannabinoids modulate ORNs activity respectively in axolotls (48) and in xenopus (49). In mammals, several neurotransmitters and hormones modulate ORNs activity (50–53), but none of them are directly related to nutritional status.

As circulating insulin rapidly increases after food intake period, we tried to mimic such an increase in the insulin environment of the OM. Insulin application on the OM rapidly and reversibly decreased EOG responses to odorants. This result provides the first

evidence of a modulation of odour detection in the OM by a metabolism-related hormone in mammals. We observed an approximately 30% reduction in the EOG signal compared to the control treatment. Such a reduction is similar to the modulation of chemosensory neurones observed in other species (45, 46, 48). It is also consistent with the reduction in odour detection demonstrated in satiated animals concomitant with the postprandial rise in circulating insulin levels (54). Insulin altered the amplitudes but not the kinetics of EOG responses. It is generally proposed that EOG amplitudes reflect the number of responding neurones and the efficiency of the signal transduction in the ORNs. By contrast, the EOG kinetics may reflect additional mechanisms involving, among others, non-neuronal cells, mucus composition or air flow rate (55, 56). Therefore, we propose that the selective inhibitory effect of insulin on the EOG amplitudes is most probably due to a direct modulation of the ORN activity. Patch-clamp recordings of ORNs in the presence of different concentrations of insulin would certainly help to unravel the mechanisms underlying the action of this hormone in the OM.

In conclusion, the present study strongly suggests the implication of insulin in the OM physiology through two pathways: a prominent endocrine one under the influence of rapid variations following food intake (peripheral insulin) and a more targeted one, through autocrine/paracrine regulations by local source of this hormone. Insulin coming from the peripheral circulation may finely tune the first step of odour detection at the OM level, thus further linking olfaction to the nutritional status of an animal. In addition, classical insulin roles, such as cell growth and survival, could be under the influences of both insulin sources.

Acknowledgements

This work was carried out with the financial support of the 'ANR – Agence Nationale de la Recherche – The French National Research Agency' under the 'Programme National de Recherche en Alimentation et nutrition humaine', project 'ANR-05-PNRA-1.E7 AROMALIM'. We thank Dr J. E. Schwob for the supply of GBC2 antibody, and Dr R. Scharfmann for Pdx1 antibody supply and for useful discussion. We are also grateful to Frédérique Perrin for help with the EOG experiments and Dr P. Lucas for help with the EOG materials. We thank the MIMA2 platform for access to the confocal microscopy equipment and UEAR (Jouy-en Josas) for animal care.

Received: 14 March 2008,
revised 27 June 2008,
accepted 2 July 2008

References

1 Berthoud HR. Interactions between the 'cognitive' and 'metabolic' brain in the control of food intake. *Physiol Behav* 2007; **91**: 486–498.
2 Bruning JC, Gautam D, Burks DJ, Gillette J, Schubert M, Orban PC, Klein R, Krone W, Muller-Wieland D, Kahn CR. Role of brain insulin receptor in control of body weight and reproduction. *Science* 2000; **289**: 2122–2125.
3 Havrankova J, Roth J, Brownstein M. Insulin receptors are widely distributed in the central nervous system of the rat. *Nature* 1978; **272**: 827–829.
4 Mulligan C, Moreau K, Brandolini M, Livingstone B, Beaufrere B, Boirie Y. Alterations of sensory perceptions in healthy elderly subjects during fasting and refeeding. A pilot study. *Gerontology* 2002; **48**: 39–43.
5 O'Doherty J, Rolls ET, Francis S, Bowtell R, McGlone F, Kobal G, Renner B, Ahne G. Sensory-specific satiety-related olfactory activation of the human orbitofrontal cortex. *Neuroreport* 2000; **11**: 893–897.
6 Hardy AB, Aioun J, Baly C, Julliard KA, Caillol M, Salesse R, Duchamp-Viret P. Orexin A modulates mitral cell activity in the rat olfactory bulb: patch-clamp study on slices and immunocytochemical localization of orexin receptors. *Endocrinology* 2005; **146**: 4042–4053.
7 Cain DP. Effects of insulin injection on responses of olfactory bulb and amygdala single units to odors. *Brain Res* 1975; **99**: 69–83.
8 Fadool DA, Tucker K, Phillips JJ, Simmen JA. Brain insulin receptor causes activity-dependent current suppression in the olfactory bulb through multiple phosphorylation of Kv1.3. *J Neurophysiol* 2000; **83**: 2332–2348.
9 Caillol M, Aioun J, Baly C, Persuy MA, Salesse R. Localization of orexins and their receptors in the rat olfactory system: possible modulation of olfactory perception by a neuropeptide synthetized centrally or locally. *Brain Res* 2003; **960**: 48–61.
10 Baly C, Aioun J, Badonnel K, Lacroix MC, Durieux D, Schlegel C, Salesse R, Caillol M. Leptin and its receptors are present in the rat olfactory mucosa and modulated by the nutritional status. *Brain Res* 2007; **1129**: 130–141.
11 Badonnel K, Denis JB, Caillol M, Monnerie R, Piumi F, Potier MC, Salesse R, Baly C. Transcription profile analysis reveals that OBP-1F mRNA is downregulated in the olfactory mucosa following food deprivation. *Chem Senses* 2007; **32**: 697–710.
12 Beites CL, Kawauchi S, Crocker CE, Calof AL. Identification and molecular regulation of neural stem cells in the olfactory epithelium. *Exp Cell Res* 2005; **306**: 309–316.
13 Mosthaf L, Grako K, Dull TJ, Coussens L, Ullrich A, McClain DA. Functionally distinct insulin receptors generated by tissue-specific alternative splicing. *EMBO J* 1990; **9**: 2409–2413.
14 Duvillie B, Attali M, Aiello V, Quemeneur E, Scharfmann R. Label-retaining cells in the rat pancreas: location and differentiation potential *in vitro*. *Diabetes* 2003; **52**: 2035–2042.
15 Chen X, Fang H, Schwob JE. Multipotency of purified, transplanted globose basal cells in olfactory epithelium. *J Comp Neurol* 2004; **469**: 457–474.
16 Feron F, MackaySim A, Andrieu JL, Matthaei KI, Holley A, Sicard G. Stress induces neurogenesis in non-neuronal cell cultures of adult olfactory epithelium. *Neuroscience* 1999; **88**: 571–583.
17 Peterson GL. A simplification of the protein assay method of Lowry *et al.* which is more generally applicable. *Anal Biochem* 1977; **83**: 346–356.
18 Scott JW, Brierley T. A functional map in rat olfactory epithelium. *Chem Senses* 1999; **24**: 679–690.
19 Reuter D, Zierold K, Schroder WH, Frings S. A depolarizing chloride current contributes to chemoelectrical transduction in olfactory sensory neurons in situ. *J Neurosci* 1998; **18**: 6623–6630.
20 Goldstein BJ, Dudley AL. The rat insulin receptor: primary structure and conservation of tissue-specific alternative messenger RNA splicing. *Mol Endocrinol* 1990; **4**: 235–244.
21 Baskin DG, Schwartz MW, Sipols AJ, D'Alessio DA, Goldstein BJ, White MF. Insulin receptor substrate-1 (IRS-1) expression in rat brain. *Endocrinology* 1994; **134**: 1952–1955.
22 Taguchi A, Wartschow LM, White MF. Brain IRS2 signaling coordinates life span and nutrient homeostasis. *Science* 2007; **317**: 369–372.
23 Torlinska T, Mackowiak P, Nogowski L, Nowak KW, Madry E, Perz M. Characteristics of insulin receptor binding to various rat tissues. *J Physiol Pharmacol* 1998; **49**: 261–270.

24 Hussar P, Tserentsoodol N, Koyama H, Yokoo-Sugawara M, Matsuzaki T, Takami S, Takata K. The glucose transporter GLUT1 and the tight junction protein occludin in nasal olfactory mucosa. *Chem Senses* 2002; **27**: 7–11.

25 Banks WA, Kastin AJ, Pan W. Uptake and degradation of blood-borne insulin by the olfactory bulb. *Peptides* 1999; **20**: 373–378.

26 Lomedico P, Rosenthal N, Efstratidadis A, Gilbert W, Kolodner R, Tizard R. The structure and evolution of the two nonallelic rat preproinsulin genes. *Cell* 1979; **18**: 545–558.

27 Cunha DA, Carneiro EM, Alves Mde C, Jorge AG, de Sousa SM, Boschero AC, Saad MJ, Velloso LA, Rocha EM. Insulin secretion by rat lacrimal glands: effects of systemic and local variables. *Am J Physiol Endocrinol Metab* 2005; **289**: E768–E775.

28 von Eggelkraut-Gottanka R, Beck-Sickinger AG. Biosynthesis of peptide hormones derived from precursor sequences. *Curr Med Chem* 2004; **11**: 2651–2665.

29 Havrankova J, Schmechel D, Roth J, Brownstein M. Identification of insulin in rat brain. *Proc Natl Acad Sci USA* 1978; **75**: 5737–5741.

30 Herrera MT, Prieto JC, Guerrero JM, Goberna R. Effects of fasting and refeeding on insulin binding to liver plasma membranes and hepatocytes from normal rats. *Horm Metab Res* 1981; **13**: 441–445.

31 Saito A, Williams JA, Goldfine ID. Alterations in brain cholecystokinin receptors after fasting. *Nature* 1981; **289**: 599–600.

32 Marks JL, Eastman CJ. Effect of starvation on insulin receptors in rat brain. *Neuroscience* 1989; **30**: 551–556.

33 Komori T, Morikawa Y, Tamura S, Doi A, Nanjo K, Senba E. Subcellular localization of glucose transporter 4 in the hypothalamic arcuate nucleus of ob/ob mice under basal conditions. *Brain Res* 2005; **1049**: 34–42.

34 Sanz C, Roncero I, Vazquez P, Navas MA, Blazquez E. Effects of glucose and insulin on glucokinase activity in rat hypothalamus. *J Endocrinol* 2007; **193**: 259–267.

35 Leibiger B, Leibiger IB, Moede T, Kemper S, Kulkarni RN, Kahn CR, de Vargas LM, Berggren PO. Selective insulin signaling through A and B insulin receptors regulates transcription of insulin and glucokinase genes in pancreatic beta cells. *Mol Cell* 2001; **7**: 559–570.

36 Calof AL, Hagiwara N, Holcomb JD, Mumm JS, Shou J. Neurogenesis and cell death in olfactory epithelium. *J Neurobiol* 1996; **30**: 67–81.

37 Cowan CM, Thai J, Krajewski S, Reed JC, Nicholson DW, Kaufmann SH, Roskams AJ. Caspases 3 and 9 send a pro-apoptotic signal from synapse to cell body in olfactory receptor neurons. *J Neurosci* 2001; **21**: 7099–7109.

38 Denley A, Wallace JC, Cosgrove LJ, Forbes BE. The insulin receptor isoform exon 11- (IR-A) in cancer and other diseases: a review. *Horm Metab Res* 2003; **35**: 778–785.

39 McEntire JK, Pixley SK. Olfactory receptor neurons in partially purified epithelial cell cultures: comparison of techniques for partial purification and identification of insulin as an important survival factor. *Chem Senses* 2000; **25**: 93–101.

40 Mielke JG, Wang YT. Insulin exerts neuroprotection by counteracting the decrease in cell-surface GABA receptors following oxygen-glucose deprivation in cultured cortical neurons. *J Neurochem* 2005; **92**: 103–113.

41 Duarte AI, Proenca T, Oliveira CR, Santos MS, Rego AC. Insulin restores metabolic function in cultured cortical neurons subjected to oxidative stress. *Diabetes* 2006; **55**: 2863–2870.

42 Vicario-Abejon C, Yusta-Boyo MJ, Fernandez-Moreno C, de Pablo F. Locally born olfactory bulb stem cells proliferate in response to insulin-related factors and require endogenous insulin-like growth factor-I for differentiation into neurons and glia. *J Neurosci* 2003; **23**: 895–906.

43 McCurdy RD, Feron F, McGrath JJ, Mackay-Sim A. Regulation of adult olfactory neurogenesis by insulin-like growth factor-I. *Eur J Neurosci* 2005; **22**: 1581–1588.

44 Hillebrand JJ, de Wied D, Adan RA. Neuropeptides, food intake and body weight regulation: a hypothalamic focus. *Peptides* 2002; **23**: 2283–2306.

45 Meunier N, Belgacem YH, Martin JR. Regulation of feeding behaviour and locomotor activity by takeout in Drosophila. *J Exp Biol* 2007; **210**: 1424–1434.

46 Kawai K, Sugimoto K, Nakashima K, Miura H, Ninomiya Y. Leptin as a modulator of sweet taste sensitivities in mice. *Proc Natl Acad Sci USA* 2000; **97**: 11044–11049.

47 Kitagawa J, Shingai T, Kajii Y, Takahashi Y, Taguchi Y, Matsumoto S. Leptin modulates the response to oleic acid in the pharynx. *Neurosci Lett* 2007; **423**: 109–112.

48 Mousley A, Polese G, Marks NJ, Eisthen HL. Terminal nerve-derived neuropeptide y modulates physiological responses in the olfactory epithelium of hungry axolotls (*Ambystoma mexicanum*). *J Neurosci* 2006; **26**: 7707–7717.

49 Czesnik D, Schild D, Kuduz J, Manzini I. Cannabinoid action in the olfactory epithelium. *Proc Natl Acad Sci USA* 2007; **104**: 2967–2972.

50 Bouvet JF, Delaleu JC, Holley A. The activity of olfactory receptor cells is affected by acetylcholine and substance P. *Neurosci Res* 1988; **5**: 214–223.

51 Kawai F, Kurahashi T, Kaneko A. Adrenaline enhances odorant contrast by modulating signal encoding in olfactory receptor cells. *Nat Neurosci* 1999; **2**: 133–138.

52 Vargas G, Lucero MT. Dopamine modulates inwardly rectifying hyperpolarization-activated current (Ih) in cultured rat olfactory receptor neurons. *J Neurophysiol* 1999; **81**: 149–158.

53 Hegg CC, Greenwood D, Huang W, Han P, Lucero MT. Activation of purinergic receptor subtypes modulates odor sensitivity. *J Neurosci* 2003; **23**: 8291–8301.

54 Aime P, Duchamp-Viret P, Chaput MA, Savigner A, Mahfouz M, Julliard AK. Fasting increases and satiation decreases olfactory detection for a neutral odor in rats. *Behav Brain Res* 2007; **179**: 258–264.

55 Scott JW, Scott-Johnson PE. The electroolfactogram: a review of its history and uses. *Microsc Res Tech* 2002; **58**: 152–160.

56 Scott JW, Acevedo HP, Sherrill L. Effects of concentration and sniff flow rate on the rat electroolfactogram. *Chem Senses* 2006; **31**: 581–593.

57 Serrano R, Villar M, Martinez C, Carrascosa JM, Gallardo N, Andres A. Differential gene expression of insulin receptor isoforms A and B and insulin receptor substrates 1, 2 and 3 in rat tissues: modulation by aging and differentiation in rat adipose tissue. *J Mol Endocrinol* 2005; **34**: 153–161.

58 Ugleholdt R, Poulsen ML, Holst PJ, Irminger JC, Orskov C, Pedersen J, Rosenkilde MM, Zhu X, Steiner DF, Holst JJ. Prohormone convertase 1/3 is essential for processing of the glucose-dependent insulinotropic polypeptide precursor. *J Biol Chem* 2006; **281**: 11050–11057.

59 Burns CJ, Minger SL, Hall S, Milne H, Ramracheya RD, Evans ND, Persaud SJ, Jones PM. The *in vitro* differentiation of rat neural stem cells into an insulin-expressing phenotype. *Biochem Biophys Res Commun* 2005; **326**: 570–577.

60 Egea JC, Hirtz C, Gross R, Lajoix AD, Traskawka E, Ribes G, de Periere DD. Preproinsulin I and II mRNA expression in adult rat submandibular glands. *Eur J Oral Sci* 2000; **108**: 292–296.

61 Nakajima-Nagata N, Sakurai T, Mitaka T, Katakai T, Yamato E, Miyazaki J, Tabata Y, Sugai M, Shimizu A. *In vitro* induction of adult hepatic progenitor cells into insulin-producing cells. *Biochem Biophys Res Commun* 2004; **318**: 625–630.